NAVAL POSTGRADUATE SCHOOL
MONTEREY, CALIFORNIA

THESIS

PARTICULATE SIZING IN GAS TURBINE EXHAUSTS USING A LASER EXTINCTION TECHNIQUE

by

Philip H. Turner

December, 1995

Thesis Advisor: Oscar Biblarz
Co-Advisor David W. Netzer

Approved for public release; distribution is unlimited.

REPORT DOCUMENTATION PAGE

Form Approved OMB No. 0704-0188

1. AGENCY USE ONLY *(Leave blank)*	2. REPORT DATE December 1995	3. REPORT TYPE AND DATES COVERED Master's Thesis

4. TITLE AND SUBTITLE PARTICULATE SIZING IN GAS TURBINE EXHAUST USING A LASER EXTINCTION TECHNIQUE

5. FUNDING NUMBERS N0042194 WR 01539

6. AUTHOR(S) Turner, Philip H.

7. PERFORMING ORGANIZATION NAME(S) AND ADDRESS(ES)
Naval Postgraduate School
Monterey CA 93943-5000

8. PERFORMING ORGANIZATION REPORT NUMBER

9. SPONSORING/MONITORING AGENCY NAME(S) AND ADDRESS(ES)
Naval Air Warfare Center, Aircraft Division, Trenton N.J.

10. SPONSORING/MONITORING AGENCY REPORT NUMBER

11. SUPPLEMENTARY NOTES The views expressed in this thesis are those of the author and do not reflect the official policy or position of the Department of Defense or the U.S. Government.

12a. DISTRIBUTION/AVAILABILITY STATEMENT
Approved for public release; distribution is unlimited.

12b. DISTRIBUTION CODE

13. ABSTRACT *(maximum 200 words)* The measurement of soot particulates densities in gas turbine engine and rocket exhausts is an area of continuing scientific investigation. Knowledge of exhaust plume soot concentration and sizing is critical for plume signature determination, currently a focus of theatre ballistic missile defense research. This thesis research investigates the development and initial calibration of an instrument that will determine soot particle densitites in an exhaust plume, by measuring the absorbtion of a light beam transmitted through the plume. This instrument utilizes an argon ion laser, four passes through the exhaust plume, and a phase conjugate crystal to correct for aberrations in the transmitted beam. Several aspects of instrument layout and performance were investigated, and an initial calibration against a conventional probe sampling technique was performed, using an ethelyne- air combustor as a soot source. While soot concentration measurements obtained with the instrument were internally consistent, the primitive sample probe used limited the opportunity to do an accurate comparison against a conventional method. The method requires further development, but shows significant promise for use in a jet engine test cell.

14. SUBJECT TERMS Coherence Length, Photrefractive Effect, Barium Titanate, Self-Pumped Phase Conjugation, Particulate Sizing			15. NUMBER OF PAGES 76 16. PRICE CODE
17. SECURITY CLASSIFICATION OF REPORT Unclassified	18. SECURITY CLASSIFICATION OF THIS PAGE Unclassified	19. SECURITY CLASSIFICATION OF ABSTRACT Unclassified	20. LIMITATION OF ABSTRACT UL

NSN 7540-01-280-5500

Standard Form 298 (Rev. 2-89)
Prescribed by ANSI Std. 239-18 298-102

Approved for public release; distribution is unlimited.

PARTICULATE SIZING IN GAS TURBINE EXHAUSTS USING A LASER EXTINCTION TECHNIQUE

Philip H. Turner
Lieutenant, United States Navy
B.S., United States Naval Academy, 1989

Submitted in partial fulfillment
of the requirements for the degree of

MASTER OF SCIENCE IN ASTRONAUTICAL ENGINEERING

from the

NAVAL POSTGRADUATE SCHOOL
December 1995

Author: _____
Philip H. Turner

Approved by: _____
Oscar Biblarz, Thesis Advisor

_____
David Netzer, Co-Advisor

_____
Daniel J. Collins, Chairman
Department of Aeronautics and Astronautics

ABSTRACT

The measurement of soot particulates densities in gas turbine engine and rocket exhausts is an area of continuing scientific investigation. Knowledge of exhaust plume soot concentration and sizing is critical for plume signature determination, currently a focus of theatre ballistic missile defense research. This thesis research investigates the development and initial calibration of an instrument that will determine soot particle densitites in an exhaust plume, by measuring the absorbtion of a light beam transmitted through the plume. This instrument utilizes an argon ion laser, four passes through the exhaust plume, and a phase conjugate crystal to correct for aberrations in the transmitted beam. Several aspects of instrument layout and performance were investigated, and an initial calibration against a conventional probe sampling technique was performed, using an ethelyne- air combustor as a soot source. While soot concentration measurements obtained with the instrument were internally consistent, the primitive sample probe used limited the opportunity to do an accurate comparison against a conventional method. The method requires further development, but shows significant promise for use in a jet engine test cell.

TABLE OF CONTENTS

ACKNOWLEDGEMENTS

I wish to thank Professor Oscar Biblarz and Professor David Netzer for their encouragement, support, and guidance throughout my research. I also wish to thank Mr. Harry Connor for the invaluable assistance he provided during the setup and experimentation involved with this thesis. I would also like to extend my appreciation to Mr. William Vorhees of the Naval Air Warfare Center, Aircraft Division, Trenton N.J., for funding this research. Finally, I am especially grateful to my wife Alysse for her unfailing support and patience during my studies at the Naval Postgraduate School. Without her support and love, this document would not exist.

I. INTRODUCTION

Engines that burn hydrocarbon fuels with oxygen or air produce significant quantities of soot as a product of combustion. This soot flows out the back of the combustion chamber in either a conventional jet engine or a hydrocarbon-fueled rocket and leaves the engine as part of the exhaust plume. Once in the exhaust plume, the soot particles will cool and can coalesce into larger particles as they travel away from the engine. Understanding the exact mechanics of this process is important for several reasons. The size and concentration of these exhaust plume soot particles has been found to significantly affect the plume heat signature. In the case of theater ballistic missiles (TBMs), accurate knowledge of the signatures is critical to launch sensing and confirmation. This problem has received increasing attention in the past five years due to the proliferation of hydrocarbon fueled TBM's. Accurate determination of exhaust plume soot concentration is also critical for pollution monitoring and verifying that local ambient air quality standards are satisfied.

Several methods have been tried in an attempt to accurately measure soot concentration in an exhaust plume, including isokinetic sampling, light extinction, single particle counters, and light scattering. Due to the high temperatures and flow velocities present in engine exhausts, many of these approaches have been difficult to transfer to a working instrument. One promising approach to this problem, reported on by Biblarz and Netzer [Ref. 1] and investigated by Glaros [Ref. 2], is the use of light extinction measurements to determine particle concentration. Extinction, the combined result of absorption and scattering, is primarily due to absorption in soot particles [Ref 1, p.4]. As soot has an "absorption coefficient" (extinction cross section q_e divided by particle mass m_p) that is relatively constant with respect to temperature and wavelength, soot mass concentration may be directly obtained [Ref. 3]. Results can then be checked against theoretical predictions based on Mie theory for light scattering by small spherical particles [Ref. 4].

This report is about the development of an instrument that utilizes laser light and a more direct method to accurately determine soot concentration in an engine test cell

environment. This instrument is unique in that it utilizes several innovative technologies, including an optical phase conjugation mirror, to minimize the effects of low obscuration, beam distortion from thermal blooming, and beam steering from density gradients, problems that have plagued previous efforts to develop such an instrument. Optical phase conjugation is a technique that incorporates nonlinear optical effects to precisely reverse both the direction of propagation and the overall phase factor for each plane wave in a beam of laser light. This allows for the near elimination of losses caused by nonuniform distorting media, referred to as the distortion correction property of phase conjugation [Ref. 5]. Use of this technology virtually eliminates light loss not caused by particle scattering and absorption, significantly increasing the potential accuracy of the instrument.

Several theoretical and practical issues are addressed in this work, including the partial correction of beam steering through the use of a retroreflector, the incomplete Phase Conjugate Mirror (PCM) distortion correction capability due to reflectivities less than unity, and an initial calibration of the instrument.

II. THEORY AND BACKGROUND

A. SOOT FORMATION

A great deal of recent research has been conducted with the goal of increasing the understanding of soot formation processes in gas turbine and rocket engines. Most of the hydrocarbon fuels used by the Navy produce soot as a byproduct of combustion. This problem is expected to become worse with the development of new high-energy fuels which have a large carbon to hydrogen ratio, leading to an increased tendency to soot [Ref. 6]. Soot reduction is a minor contributor to increased combustion efficiency, but is very important for reduced signatures from propulsion system exhausts. The recent proliferation of hydrocarbon fueled theater ballistic missiles (TBM's) has resulted in a great deal of interest in TBM infra-red plume signatures and in tracking TBM's with radar. At this time, not enough is known about soot particles in rocket exhausts and their contribution to plume radar cross section. All of these military problems highlight the need for an increased understanding of soot formation and evolution

in a combustion environment. No current first-principles soot prediction capability is available, and reaction kinetics are markedly different for air breathing jet engines and oxygen-based rockets [Ref. 7].

One of the most significant obstacles to understanding the soot formation process is the lack of a reliable, accurate method of determining soot concentration in the engine exhaust. Even after formation, soot can undergo secondary reactions in the plume, including "chemical reactions, condensation, and size evolution" that further alter its characteristics [Ref. 1, p. 3]. One challenging result of these reactions is that "particle size and shape depend on the conditions in the flame. They may be almost spherical or in the form of long filaments. The radii of these particles range from 5 to 100 nm." [Ref. 8]. This wide variation in particle shape and size has accounted for some of the difficulties faced by previous investigations of particle sizing techniques.

B. PARTICULATE SAMPLING METHODS

Aerosol sampling and analysis is normally divided into two major classes; collection-based techniques versus direct reading or *in situ* methods. Collection techniques, the traditional method of measurement, allow for extensive analysis of the particles under controlled laboratory conditions. Against this advantage, however, are the significant disadvantages that particles may be modified by the collection process and that measurement equipment is difficult to build and calibrate [Ref. 9]. Direct optical techniques offer less extensive information about particle characterization, but provide rapid response and do not disturb the process being observed. While collection techniques have been the historical standard, the rapid increases in available computing power have renewed interest in direct transmission reading measurements. For operation in a demanding high temperature, high flow rate environment such as a jet engine or rocket exhaust, direct techniques are clearly advantageous.

C. MEASUREMENT USING LASER LIGHT EXTINCTION

One subset of the direct techniques, optical measurement methods offer high sensitivity, nearly instantaneous response, and the avoidance of physical contact with the particles [Ref. 10]. Optical instruments may be either single particle counters or rely on the combined extinction and scattering effect of an ensemble of particles, which can have either monomodal or multimodal size distributions, the latter being much more difficult to interpret. Optical techniques may also be characterized by their use of either scattering or absorption as a basis for operation. These instruments must sometimes measure particles varying in size over several orders of magnitude, with physical properties that result in extinction measurements dominated by pure absorption or extinction with a significant scattering component. Either scattering or absorption based measurement instruments have been used, based on the system being studied, the size of the particles, and their composition. Scattering measurement results can also be compared with independent absorption readings as a verification of overall results.

After an overview of the fundamental principles of light scattering and absorption by particles, the current theory and its inherent limitations will be covered, followed by a description of the new extinction-based technique to be utilized by the proposed instrument.

1. Principles

Extinction may be defined as the combination of light scattering and absorption by a particle suspended in a non-absorbing medium. The ratio between these two processes is determined by three factors: the refractive index of a particle, particle size relative to the wavelength of incident light, and the polarization of this light (vertical for this instrument).

The refractive index m is defined as $m=m_1/m_2$ where m_1 is the refractive index of the particle and m_2 is the refractive index of the medium. Both refractive indices are of the form a-bi, where the real component a is the refraction coefficient of the substance and the complex component b is the absorption coefficient. Air and other relatively transparent substances have an absorption coefficient of nearly 0, while for some metals it may be almost 1 [Ref. 11]. For the carbon particles

of interest in an exhaust plume, the refractive index is roughly m≅1.50-0.6i, indicating that absorption dominates the extinction process [Ref. 12].

The size parameter α, a measure of particle size relative to the wavelength of incident radiation, is given by:

$$\alpha=\pi D/\lambda = \pi D/(\lambda_o/m_2) \qquad (2\text{-}1)$$

where:

λ = wavelength of radiation in medium

λ_o = wavelength of radiation in vacuum

m_2 = refractive index of medium

Given a size parameter for a spherical particle, the applicable mode of scattering may be determined [Ref. 4]. There are three modes which are based on the Lorenz-Mie solution to Maxwell's equations, with some simplifications possible for relatively large or small particles. For very small particles ($\alpha<<1$ or $D<\lambda/10\rightarrow$ 0.05 microns particle size for visible light), the particle experiences a uniform electric field from the incident radiation. This Rayleigh Scattering regime is characterized by a very small extinction

coefficient Q_{ext}, and a scattered intensity proportional to λ^{-4}. Particles in the Rayleigh regime have scattering functions with little or no distinct structure, and absorption is dominant in the overall extinction process. Due to these characteristics, Rayleigh scattering can only be employed successfully for soot of a known refractive index and relatively low number concentrations of particles, and with most below the $\lambda/10$ size threshold, where the effects of particle agglomeration are reduced [Ref. 16].

For relatively large particles ($\alpha>>1$ or D>5.0 microns for visible light), the wave front can be treated as a bundle of rays and geometric optics used to determine the refraction, reflection, and diffraction of the light by the particle. Refraction and reflection are highly dependent on particle shape and composition, producing unique patterns that may be used to size the particle. Diffraction is unique in that the forward lobe becomes compressed as particle size increases, becoming the major contributing process. For particles greater than 1 micron in diameter, this (Fraunhofer) diffraction dominates the near forward direction [Ref. 4, p. 104]. The extinction coefficient, Q_{ext} for transparent

particles in the geometric regime rises to a nearly constant value of two, with similar results observed for irregular absorbing particles [Ref. 1, p. 26]. Asymptotic approximations to Mie theory efficiency factors have been used by Nussenzveig and Wiscombe for particles with α ranging from 10 to 1000, with refractive indices similar to soot [Ref. 13]. These authors claim a reduction in relative errors from (1-10)% to $(10^{-2} - 10^{-3})$% using these approximations instead of geometric theory.

Between these two extremes, the complete Lorenz-Mie solutions must be used. This region produces extremely complex interactions, as the particle diameter is roughly the same magnitude as the incident radiation wavelength and is therefore experiencing a non-uniform electromagnetic field. This region is also an area of great interest for soot particulate studies. Soot particles in engine exhausts are typically considered to be log-normal polydispersions, with diameters ranging from 0.005 to 0.5 microns and with the bulk of the mass contained in the smaller sizes [Ref. 1]. For measurement using visible light, with wavelengths of approximately 0.5 microns and α ranging from 0.04 to 0.62, it

becomes apparent that most particle sizing will be done in the transition from the upper Rayleigh to Mie regimes. Scattering in the Mie regime is strongly affected by particle shape and index of refraction, with forward scattered light being the least disturbed. As mentioned above, this interaction will be almost completely dominated for soot by absorption; from Mie calculations for α equal to 0.1, the ratio of absorption to scattering would be about 1000 to 1. [Ref. 2]. For this reason, most current optical sizing schemes rely on absorption measurements.

One significant documented weakness of Mie theory for soot evaluation is the assumption present in the derivation that all particles are spherical. While some work has been done on ellipsoids, clusters of spheres, and other simple non-spherical shapes, these are of limited applicability and are frequently valid only for a limited range of refractive index values [Ref. 14]. As soot forms highly complex chains and fractal agglomerations, conventional Mie theory requires significant modification if it is to be used for soot particle sizing [Ref. 15]. Predicted Mie extinction values for aggregations have only agreed with experimental values when

significant changes are made in the assumed refractive index of the particle agglomerate [Ref. 16]. Departures from sphericity and uncertainties in the refractive index are considered to be the main impediments to "reliable interpretation of the measurements in terms of the properties of the soot aerosol" [Ref. 17, p. 208].

2. Extinction Measurements

All of the above methods assume that the particles are spaced more than several particle diameters apart so that each interaction may be treated as a single event. Assuming this condition is satisfied, which is true in all soot concentrations likely to be encountered in an engine exhaust, the overall light transmission through a particle cloud is given by the Beer-Lambert law [Ref. 18]:

$$T=\exp(-QA\eta L) = \exp[-(3QC_M L/2\rho D)] \qquad (2\text{-}2)$$

where: T = fraction of light transmitted,
Q = dimensionless extinction coefficient,
A = cross sectional area of the particle,
η = number concentration of particles
L = path length,

C_M = mass concentration of the particles

ρ = particle density

D = particle diameter

This has since been revised by Dobbins to include polydisperse systems of particles, using

$$T=\exp[-(3Q_{avg}C_ML/2\rho D_{32})] \qquad (2\text{-}3)$$

where Q_{avg} is an average extinction coefficient and D_{32} is the volume-to-surface or Sauter mean diameter [Ref. 17], defined as:

$$D_{32} = \frac{\int p(D)\, D^3 dD}{\int p(D)\, D^2 dD} \qquad (2\text{-}4)$$

where p(D) is the number of particles with a given diameter D. The concept of the Sauter mean diameter can be used to describe nonspherical objects, while preserving the volume to surface relation. Unfortunately, there is no guarantee that Mie calculations using this D_{32} will be even internally consistent due to the non-linearities present in Mie theory [Ref. 1, p. 7]. One significant problem is that of bimodal size distributions; in this case "even a small percentage of

larger particles will carry most of the mass and scatter/absorb the most" [Ref. 1, p. 5].

D. CURRENT STATUS

The advantages of optical systems for soot measurement have made them the object of a significant research effort, aimed at bringing the technology out of the laboratory and into a test cell environment. Present methods depend on determining an equivalent Sauter mean diameter of the particle distribution, a complicated process based on Mie solutions and probability theory [Ref. 18]. This approach is tenuous as it assumes an equivalent spherical diameter for irregularly shaped particles that may even be present in a bimodal distribution. Probability density functions are based on experimental sampling results, with no independent verification of accuracy. Because of these limitations, most current experiments have "not shown good agreement of transmission values with the theory based on Mie spheres" [Ref. 1, p. 7]. Another disadvantage of this approach is that it necessitates the use of simultaneous multi-wavelength measurements and the comparison of ratios between

measurements. While a minimum of three wavelengths are required [Ref. 18], more are often used, complicating the equipment design and calibration significantly. Some methods have also relied upon scattered light, which in addition to being relatively weak compared to absorbed light, is highly sensitive in the Mie regime to particle size, refractive index, and configuration.

E. THEORETICAL APPROACH

The current investigation is based on the approach outlined by Biblarz and Netzer [Ref. 1], and on the soot extinction properties described in section C. This approach relies upon the use of an "absorption coefficient" (μ_e), defined as:

$$\mu_e = \frac{q_e N}{C_m} = \left(\frac{3}{2}\right) \frac{Q_e}{\rho_p d} \qquad (2\text{-}5)$$

where:

q_e = extinction cross section

Q_E = efficiency factor

N = number density of the soot particles

C_m = desired mass concentration

ρ_p = particle density

This parameter has the great advantage that it is a function only of the wavelength and the soot material properties and is largely unaffected by the variations in configuration of the complex soot agglomerates described above. A second order polynomial can be used to describe the wavelength dependance of μ_e. This polynomial is then evaluated by taking multiple-wavelength measurements and comparing the ratios at different wavelengths. From previous theoretical work [Ref. 1, p. 16], the empirical absorption coefficient value can be taken to be

$$\mu_e \approx 5000\, m^2/kg \text{ for } \lambda = 300\text{-}700\, nm \qquad (2\text{-}6)$$

This value will be used for the experimental investigation. The total transmission ratio is given by

$$T = \exp\left[-\alpha_e L_e\right] = \frac{(I/I_o)\, with\, flow}{(I/I_o)\, without\, flow} \qquad (2\text{-}7)$$

where: α_e - extinction coefficient

L_e - extinction pathlength

The total soot mass flow rate out of the combustor is then given by:

$$\dot{m} = C_m AV = AV\ln(1/T)/(\mu_e L_e) \qquad (2\text{-}8)$$

where: A = cross sectional area of the plume

C_m = soot mass concentration

V = mass mean velocity of the flow

With the temperature and velocity of the exhaust gas known, the soot mass flow rate may then be calculated from the transmittance. One great advantage of this approach is that no Sauter mean diameters are required, only a reference parameter to distinguish soot from other particles in the plume. This approach, based on extinction measurements while avoiding the specific use of the complex index of refraction, has already shown good agreement with predicted values of the absorption coefficient based on Mie theory [Ref. 2, p. 1].

F. OPTICAL PHASE CONJUGATION

One unique feature of the proposed instrument is the use of an optical phase conjugate mirror to reduce beam losses not due to attenuation by soot. Optical phase conjugators are a class of materials that can produce a unique nonlinear optical

effect, where an incident beam of light produces a time-reversed replica along the path of incidence. This wavefront-reversed beam is the complex conjugate of the original beam and gives rise to a number of unique opportunities for optical processing.

Several substances are capable of producing phase conjugate waves through a variety of processes, including the inelastic effects of stimulated Brillouin scattering and stimulated Raman scattering as well as the elastic effect of optical four-wave mixing in third-order non-linear materials [Ref. 19]. By far the most efficient, however, are the photorefractive conjugators, materials with an minimum intensity requirement of only 1 W/cm^2 for operation [Ref. 20]. These materials, where the "presence of an optical interference pattern in a material can modify the refractive index via the electro-optic effect" are some of the most sensitive discovered to date for performing phase conjugation [Ref. 21, p. 55]. Phase conjugation in photorefractive materials occurs when electric charges trapped in the material migrate in the presence of light, causing a large (10^{-3}) change in the refractive index of the material [Ref. 21, p. 420].

Photorefractive materials can be externally pumped to produce this effect, but some, including $BaTiO_3$, have been demonstrated with "self pumping", where the incident beam provides the pump beams through two-beam coupling. This property is extremely desirable for the proposed instrument, as it significantly reduces the increased cost and alignment complexities inherent in the use of separate external laser pumping beams.

Distortion correction is one of the unique characteristics of optical phase conjugate mirrors (PCMs). A planar wave transmitted through a distorting medium acquires aberrations through thermal blooming, beam steering, and other distortions, as seen in Figure 2.1.

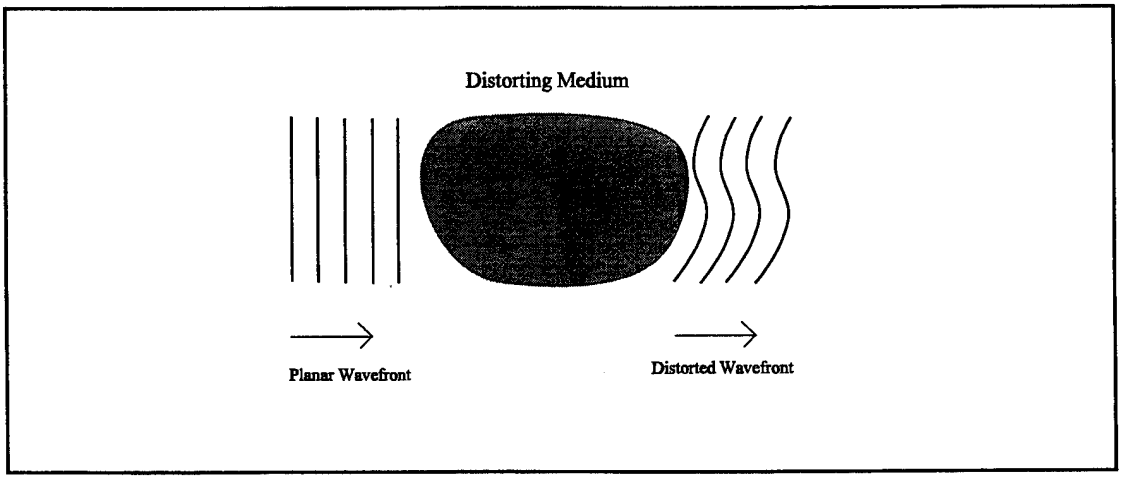

Figure 2.1 Planar Distortion

Conventional reflection will only double this distortive effect. By generating the complex conjugate and retransmitting it through the beam, however, the original waveform may be recovered, as shown in Figure 2.2.

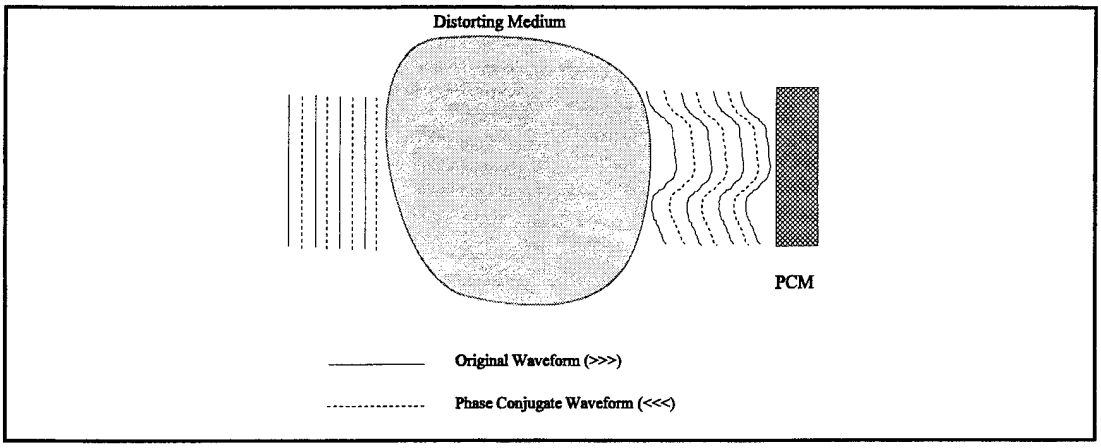

Figure 2.2 Distortion Correction with PCM

This distortion correction property depends on the generation of a true phase conjugate beam for retransmission through the distorting medium. For this replica to exist, two main conditions must be satisfied: no energy must be lost transiting the medium, and the phase conjugator must have a reflectivity of unity [Ref. 21]. For particulate analysis, some energy must be lost in the beam transmission through an exhaust plume through the extinction processes discussed earlier. The second condition, that the PCM material will ideally reflect all incident radiation, is important for

correction of incident beam aberration, as a reflectivity of unity should be used to obtain complete reversal of the distortion. Photorefractive phase conjugate mirrors can have a gain greater than one only if separate pump beams are used. Differences as small as a 0.25 mrad misalignment in the pump wave of a Degenerate Four Wave Mixing conjugator, causing reflectivity to drop to 0.83, have been shown to cause significant distortion in an image received through a double-pass technique [Ref. 21, p. 543]. The surface reflectivity of the $BaTiO_3$ crystal, estimated at 10% due to the difference in the $BaTiO_3$ index of refraction and that of air, and the imperfect internal reflection will always limit the overall reflective efficiency of the crystal to between 60-80%, with 73% previously cited [Ref. 22]. For the PCM used in the present experiments, the measured reflectivity, based on the power levels of the incident and reflected beams, is 70%. All of the above conditions will have some effect on the recovery of wave distortion and thermal blooming, and quantification of this effect was one of the experimental goals.

III. EXPERIMENTAL INVESTIGATION

A. OVERVIEW

The initial instrument design was based on the recommendations of Glaros [Ref. 1], and was set up to compare a reference beam with a scene beam that had passed through the exhaust, as shown in Figure 3.1.

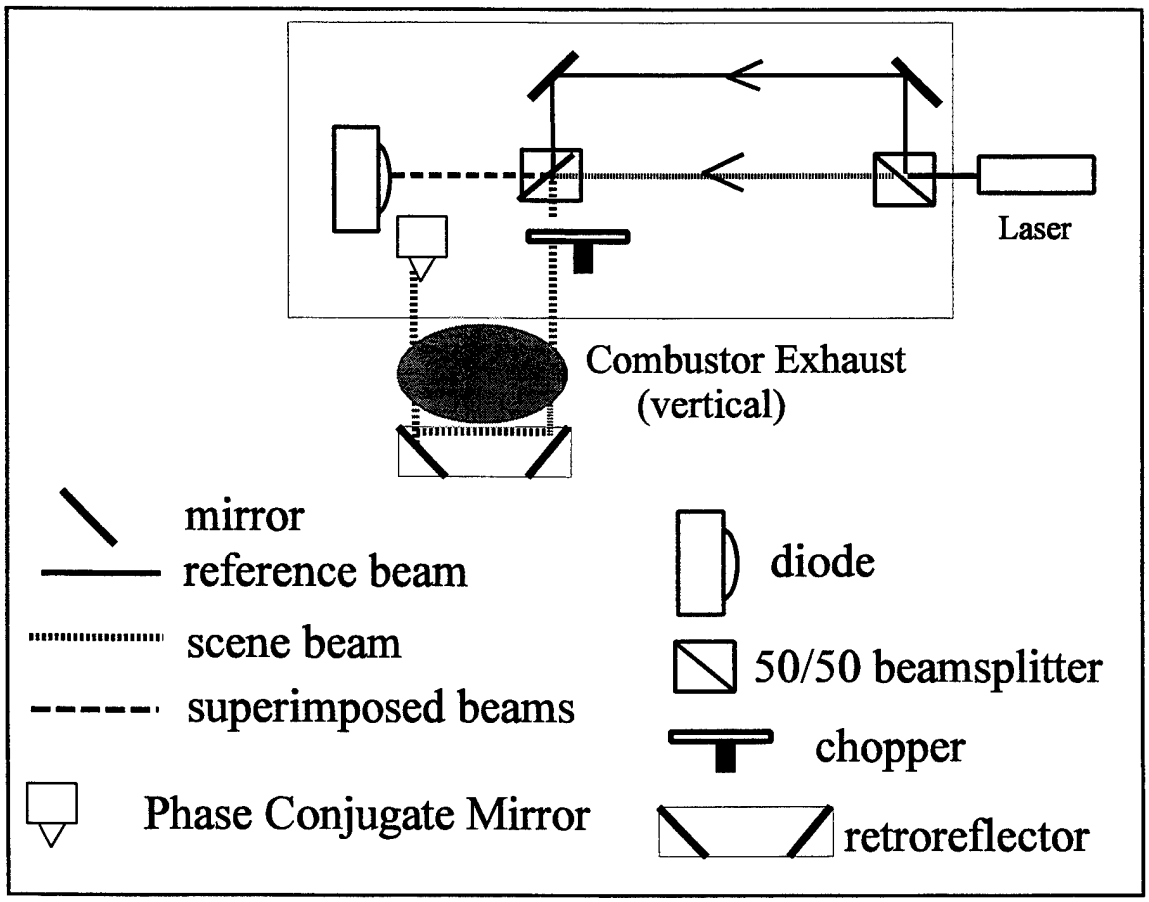

Figure 3.1 Initial Instrument Design

Overall instrument design was driven by the requirement to operate in a condition of high vibration, extreme temperatures, and potentially harmful exhaust gases. A single optical detector, measuring both the reference and scene beams, is used to eliminate drift and calibration uncertainties. All optics, with the exception of the retroreflector, are mounted on an optical breadboard to minimize vibration effects. The retroreflector is a sealed unit with replaceable quartz windows, designed to be mounted on the opposite wall of a test cell. The high speed chopper provides numerous small snapshots of the plume at a frequency above the natural resonant frequencies found in a test cell environment, further reducing variations from vibration.

Barium titanate was chosen for the phase conjugate material primarily due to the self-pumping feature and the relatively low power levels required to produce a conjugate beam. Use of a this self-pumped photorefractive material avoided the cost and pump beam alignment complexities inherent in the use of conventional four-wave mixing materials, a prime consideration for an instrument designed for the harsh environment of an engine test cell. The $BaTiO_3$ crystal used

was a 5mm x 5mm x 5 mm cube manufactured by Lockheed Sanders, with a 45° face cut relative to the primary axis (as shown in Figure 3.2) to reduce surface reflectivity and produce response times roughly one order of magnitude greater than a conventional flat cut.

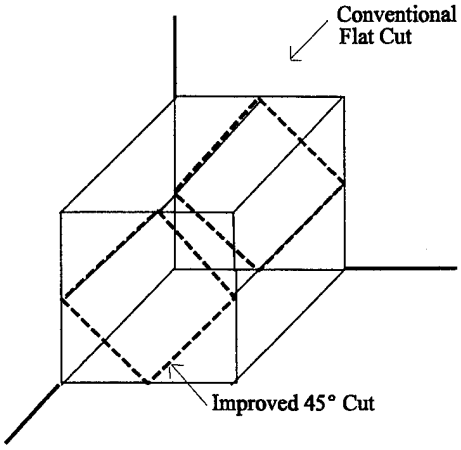

Figure 3.2 $BaTiO_3$ Geometries

A Lexel 2 Watt Argon Ion laser was used in the standard multimode setup, vertically polarized and operating in the TEM_{00} mode at a wavelength of 514.5 nm. One of the recommendations from previous investigations had been to include an intercavity etalon in order to maximize the coherence length and phase conjugate beam formation [Refs. 1,2]. The coherence length is related to the bandwidth of the

laser by:

$$l_c = c/\Delta v \qquad (3\text{-}1)$$

where Δv is the line-width of the laser. For the laser used, this distance is 0.1 meters. With the instrument setup used, the light reaching the conjugate crystal would not be coherent, and one of the experimental goals was to determine what, if any, effect this would have on the accuracy of the instrument. The laser output passes through a 50/50 cube beamsplitter, with the measurement beam split off from the reference beam. After reversing direction through two mirror reflections, necessary due to the layout of the experimental apparatus, the measurement beam passes through a second 50/50 beamsplitter. The purpose of this splitter is to allow the returning signal to enter the diode, superimposed on the reference beam. The measurement beam is modulated by an optical chopper, capable of operating between 100 and 6400 Hz. The faster speeds were normally used in order to obtain a nearly instantaneous image of the plume. After chopping, the beam passes out of the instrument, crossing the exhaust plume, and enters a Lateral Transfer Hollow Retroreflector (LTHR), manufactured by the PLX Corporation. This device offsets and

returns a beam across the plume parallel to the incident beam within 10 arc seconds for a wide range of incidence angles. A three inch offset is used to allow the OPM to be placed with the other equipment, while still giving four passes through the relatively small test plume. In an operating instrument, an offset as great as six inches could be used. After crossing the plume, the beam re-enters the instrument and is optically conjugated in the $BaTiO_3$ crystal. Returning along an identical path, the beam completes the third and fourth crossings of the plume. The reference and measurement beams are superimposed on one another and enter a photodiode that is shielded to prevent spurious scattered signals from affecting the measurements. This diode generates a reference and measurement signal for display on an oscilloscope. While an Analogic digital oscilloscope was used for this experiment, the data could easily be processed and stored on a personal computer, using a small routine written for Viewdac or similar data acquisition software.

The distortion correction principle is shown in Figure 3.3. A reference signal was obtained initially, with the diode

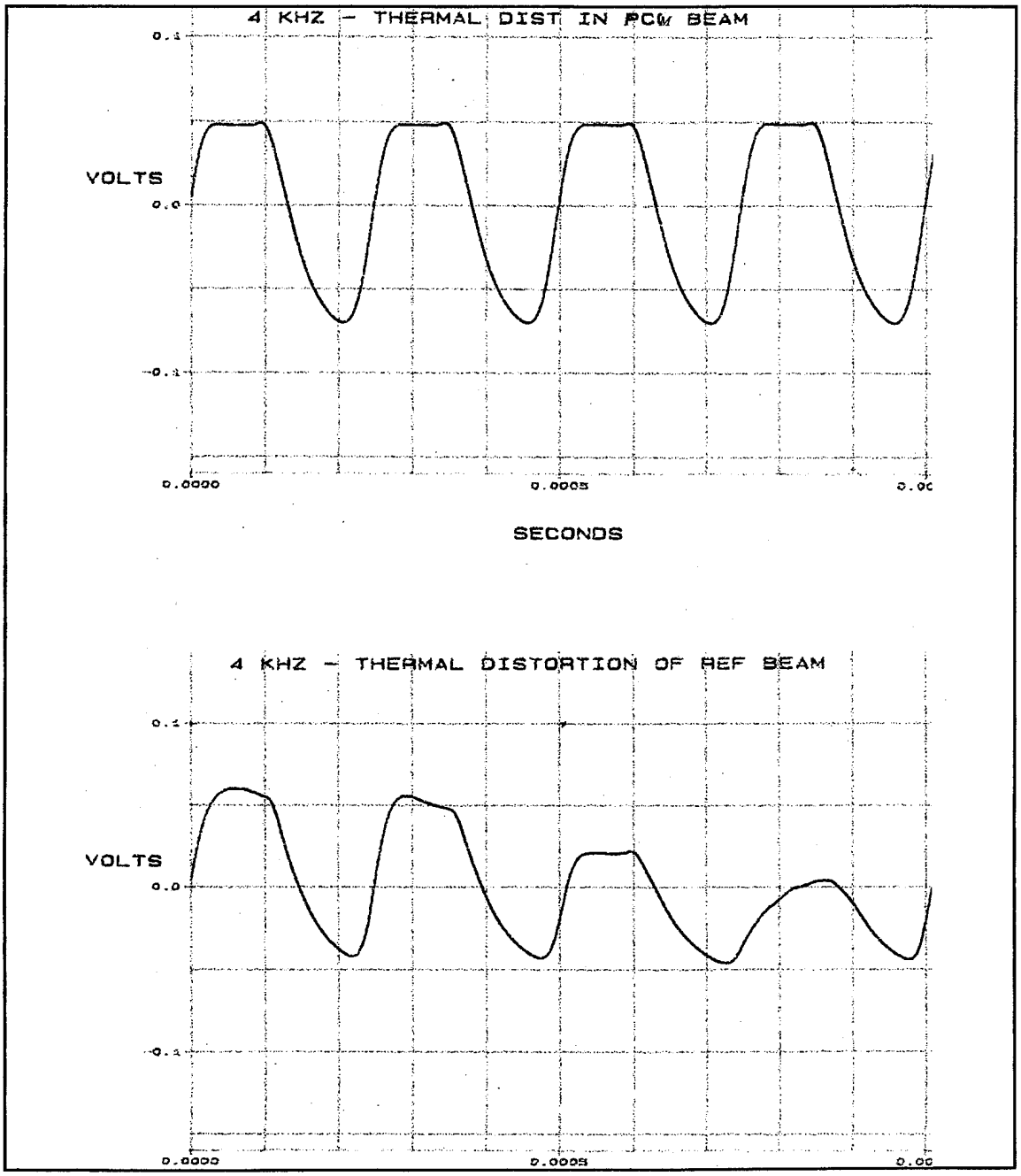

Figure 3.3 Effects of Thermal Distortion

voltage proportional to the incident light intensity. Following this, a run was made with a thermal distortion source (in this case, a source producing thermal blooming and beam steering while generating relatively little soot). As can be seen from the first figure, the square waveform was maintained. This is due to the retransmittal of the conjugate waveform and the subsequent reversal of the distorting effect. In the second figure, the distortion source was applied to the uncorrected reference beam, producing significant aberrations.

Several runs with this thermal distortion source were made in order to obtain a qualitative estimate of the effect of reflective losses on distortion correction. While reflectivities less than 1.0 have a significant effect on correction of image distortion, as discussed above, they did not appear to have as significant an effect on the recovery of a simple square waveform. While some distortion was observed, the overall waveform was largely intact after two passes through the plume. A quantitative assessment of this issue was included as one component of the experimental runs.

B. PROCEDURES

The experimental procedure was designed to begin with a verification of the Glaros [Ref. 2] results. It was followed by a more comprehensive evaluation of the instrument with a specific focus on ensuring that the fundamental processes involved were understood, with a parallel effort to perform initial calibration and increase the accuracy and utility of the design.

Beginning with a helium-neon laser, an attempt was made to generate a phase-conjugate beam using the Glaros setup shown in Figure 3.1 [Ref. 2, p. 28]. Based on previous investigations, the 8 mW helium neon laser was predicted to have sufficient power to produce photorefractive conjugation in the crystal [Ref. 2]. Experiments with the He-Ne laser showed that, while phase conjugation could be achieved, it was extremely dependant on laser alignment and chopping speed. Photorefractive phase conjugators have a demonstrated sensitivity to pumping beam intensity; as the intensity increases, the gain of the PCM remains constant but the speed of the photorefractive mirror increases [Ref. 21, p. 437]. In the self-pumped mode, the intensity of the incident beam will

determine the pump beam intensity, as two-beam coupling is being used. As this system is designed for use with a high-speed chopped signal, low power incident light can be expected to severely limit the PCM response speed. This was found to be the case with the He-Ne laser; while satisfactory for operation below several hundred Hz, the performance fell off significantly with increased chopping speeds. The argon-ion laser, operating at far higher power levels and the more desirable wavelength of 514.5 nm versus 633 nm for the He-Ne, was judged to be more suitable for the proposed design.

After verification of the results obtained by Glaros, a small combustor was set up to generate the required sooty plume for initial calibration of the instrument. The combustor burned ethylene and air with various equivalence ratios, with flowmeters and pressure gauges attached to the inlet lines in order to measure the flowrates. The flowmeters gave volumetric flow rates of the two input gases, which were converted to mass flow rates with a density correction factor (the density of air is 0.97 times the density of C_2H_4 when both gases are at identical temperatures and pressures). Cooling air was also used, being injected into a plenum outside the

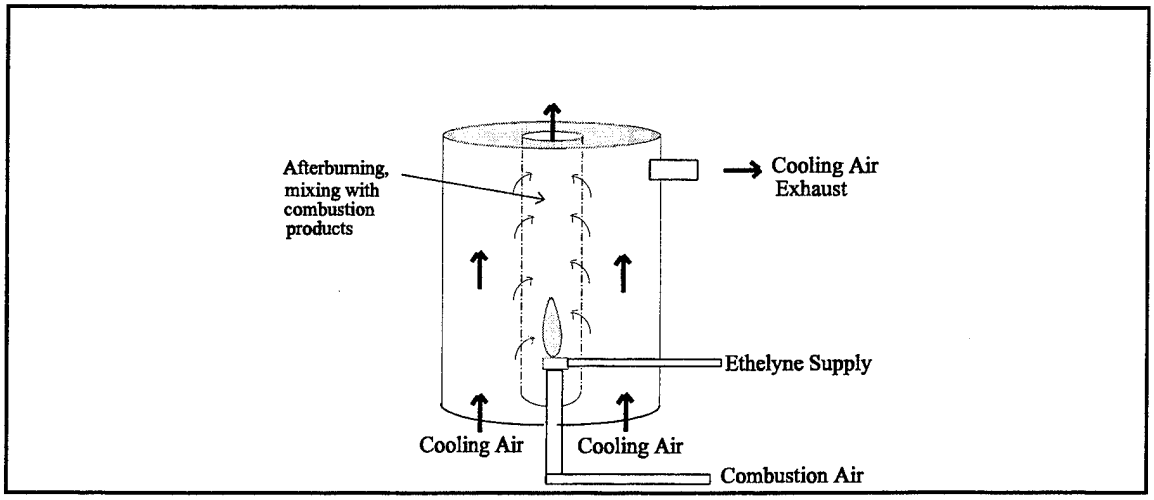

Figure 3.4 Combustor Schematic

chamber and flowing through numerous small holes in the chamber wall where it mixed with the combustion products before flowing out the nozzle or out one of two side exhaust ports, as shown in Figure 3.4

A flowmeter was used to measure the flow in the cooling air line, as it had a large effect on secondary burning of soot and on dilution of soot in the exhaust plume. While combustion air flow was also monitored, it was found to have a relatively insignificant effect on soot formation compared to the total air flow. The overall setup is shown in Figure 3.5. The combustor was enclosed in a 20.0 cm. diameter exhaust duct, with a slight negative pressure provided by a

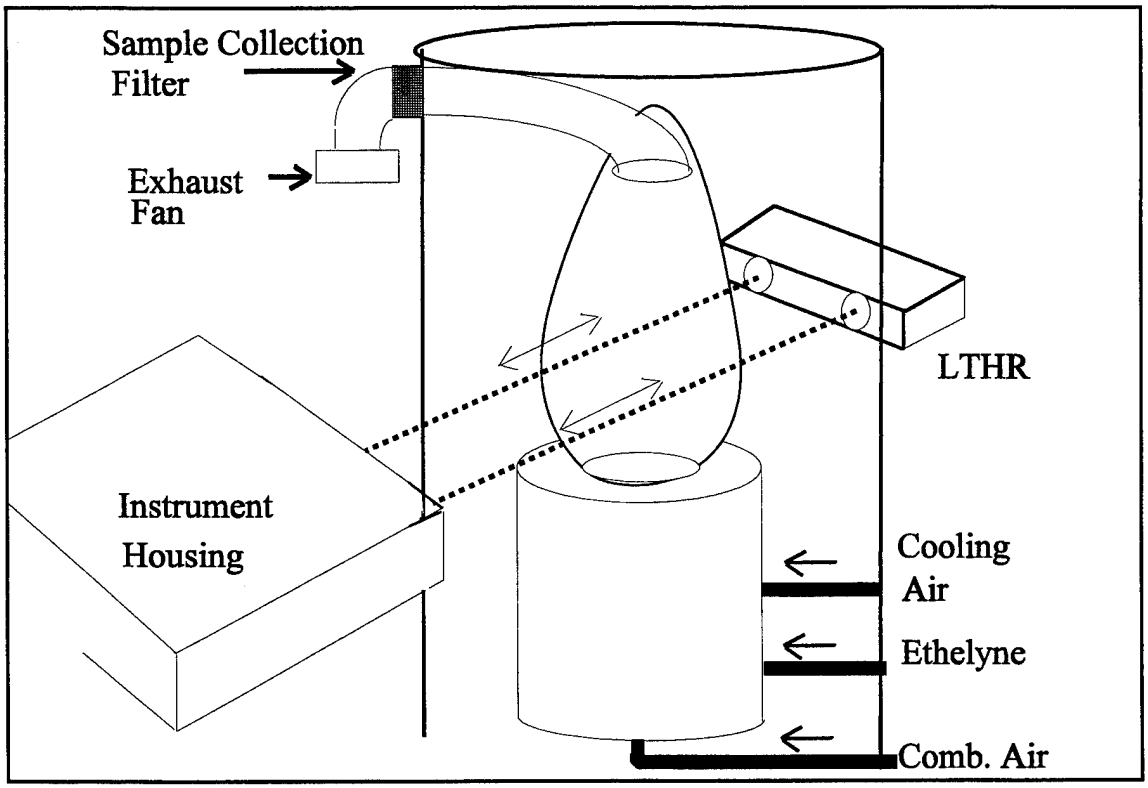

Figure 3.5 Overall experimental setup

fan to create a suction. A Millipore filter holder was placed outside the duct, with an exhaust fan attached to provide a filter airflow approximately equal to the duct airflow.

The gas sampled by the filter came from the plume through an angled inlet pipe with a 5.0 cm. diameter opening placed 30.0 cm. above the combustor and 5.0 cm. above the laser beam. The filter used was a Millipore 0.25 μm paper disc rated at 99.99% efficiency. As an initial test, three 30

minute sampling runs of the system were conducted and the samples were measured and analyzed using an electron microscope.

Mass values obtained were multiplied by 3.0 to convert the probe measurements to plume measurements, which had an area three times that of the probe at the sample point. Results were as follows:

RUN	TIME (min)	GAS VOLUMETRIC FLOW RATE (m^3/min)	COLLECTED MASS (g)	SOOT MASS FLOW RATE (kg/min)
1	30	0.691	0.005	5.01e-7
2	30	0.724	0.009	9.00e-7
3	30	0.691	0.006	6.00e-7

Table 3.1 Combustor Calibration Runs using Millipore filter

Initial runs indicated that the combustor was producing soot, but that only minute quantities of this soot were being collected for analysis. While the collected sample masses were consistent, the fact that runs of 30 minutes yielded soot mass differences of less than ten milligrams meant that accurate measurement was crucial. Electron microscope analysis of the filters for particles was not conclusive, as

particles smaller than ten microns could not be distinguished from the background filter fibers using the microscope system available. This was probably due to the very small soot quantities collected, or possibly was due to nature of the filter paper used; only agglomerations of 30 microns or greater were visible. An instrument operating in a test cell environment would collect substantially more soot, reducing this uncertainty.

The plume dimensions were analyzed with an AEGEMA 870 thermal imaging camera, and a hot wire anemometer and thermocouples were used to obtain information on the temperature, velocity, and spatial distributions. The plume was initially defined as any area of the duct more than 40 degrees above the ambient temperature. As a check on this, a traverse of the plume was done with the proposed instrument, with the 95% transmittance point taken to be the effective edge of the plume. These two methods were generally consistent, with the temperature measurements giving a plume size of 6.35 cm at the laser sampling point. Using the more accurate transmittance method, the plume size was found to be relatively smaller and relatively constant, typically starting

at slightly more than 5.1 cm in diameter at the laser sampling point and increasing to more than 8.5 cm at the filter collection point. The transmittance-based measurements were used for calculations, giving a plume area of 0.00317 m^2 and an extinction length of 0.127 m for use in converting transmittance measurements to soot mass flow rates. The overall plume was relatively cool, ranging from 300° F at the laser entry point to 160° F at the probe sampling point. While these are significantly cooler than some engines, the internal combustor temperature was still at least 1250° F, close enough to operating combustor temperatures to obtain representative samples. A more sophisticated probe sampling system would allow operation at higher temperatures. The flow velocity was measured using the anemometer at the collection probe sample point, and traversed across three points in the duct, 3 cm from each wall and once at the center. The variation between the outer and center points was between 6-9%, indicating a relatively flat velocity profile across most of the region of interest. The large duct size relative to the plume and the relatively low flow velocities involved were believed to be responsible for these characteristics. Flow

velocities were measured for different values of total air flow to ethylene flow, as the cooling air typically had a flow rate ten times that of the combustion air, producing larger effects on total exhaust velocity. Given a air mass flow/fuel mass flow ratio r of 14.7/1 as stochiometric, the combustor was set up to burn fuel rich in order to produce a sooty plume. Average velocities, as shown below, were used for calculation of soot mass flow rate.

TOTAL AIR/C_2H_4 MASS FLOW MIXTURE RATIO (r)	**EXHAUST VELOCITY (m/s)**
13.3/1	2.98
10.0/1	2.54
8.0/1	1.93
6.0/1	1.47

Table 3.2 Exhaust Flow Velocities

The time response of the PCM arrangement in the initial setup was still not as fast as reported by other investigators, with a significant drop off in intensity above 3000 Hz. The rise time was relatively rapid (typically 19-25 μs), but exact alignment was necessary to produce the square top waveform needed for intensity measurements. It was theorized that this was due to the lack of coherence length, or possibly was a function of the individual crystal used. As

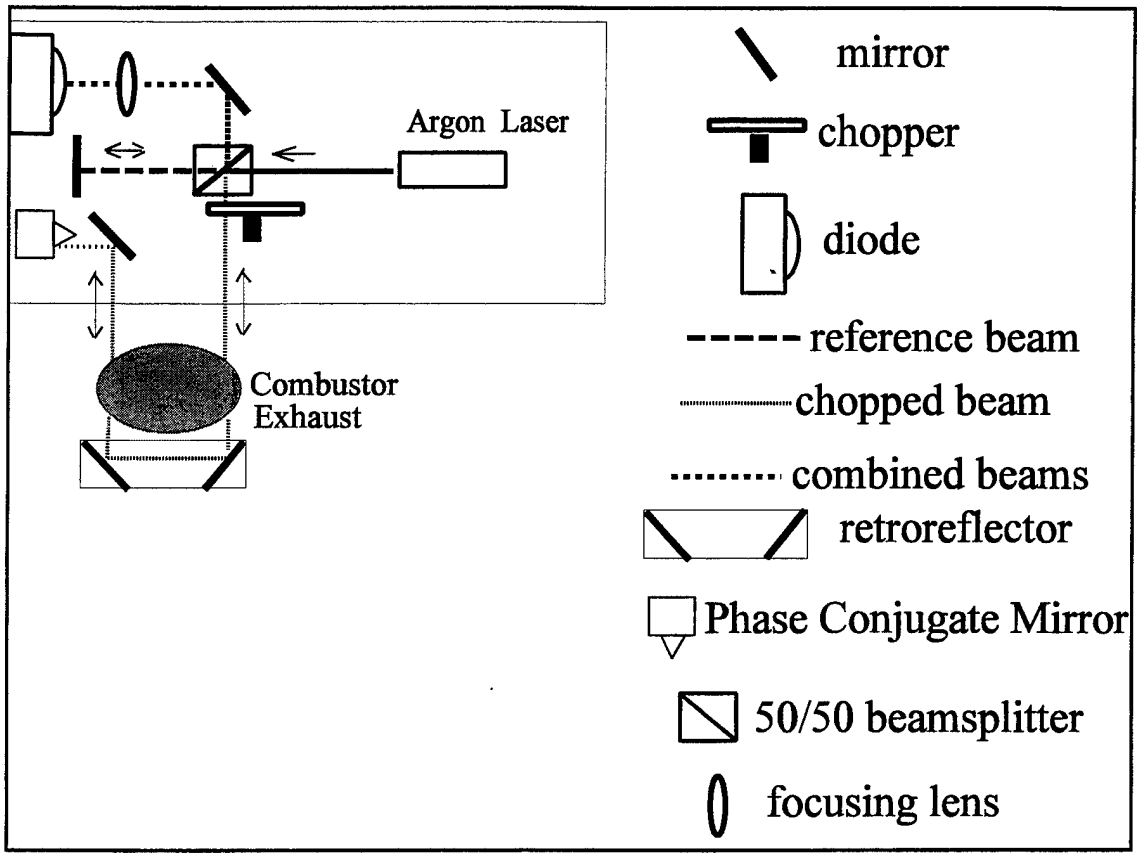

Figure 3.6 Modified Instrument Design

faster speeds are highly desirable for minimizing vibration and turbulence effects and obtaining nearly instantaneous readings on the exhaust plumes, a modified setup was used in an attempt to increase the response time. This setup, shown in Figure 3.6, eliminates one of the beam splitters and produces increased power into the PCM, which decreases the response time, produces a more accurate output waveform, and increases the diode output voltage from 70 to 105mV as seen

in Figure 3.7. The mirror just prior to the PCM ensures that vertically polarized light reaches the mirror for optimum conjugation.

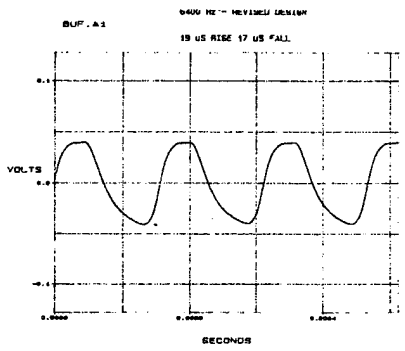

Figure 3.7 Improved performance- 6400 Hz

The differences between Figure 3.7 and an optimal square wave pattern are primarily due to the small but finite time required for phase conjugation in the PCM. This effect is barely noticeable at the lower, 2000 Hz speeds used initially. As speeds increase, this time lag has an increasing effect on the wave shape. It is still possible however, to obtain the flat top on the wave that is necessary for transmission measurements. With careful design, higher chopping speeds can be used with the instrument setup described.

Moving the chopper directly in front of the beamsplitter produced a more uniform beam. The instrument now outputs a single square top waveform, with the amplitude based on the superimposed plume and reference beams. Operation at 4000-6000 Hz was now more feasible, and the system was set up to obtain quantitative results through calibration against a filter sampling method.

IV. DISCUSSION OF RESULTS

One of the auxiliary issues addressed was verifying the laser characteristics, including determining coherence length, beam diameter and divergence, and the intensity profile across the beam. It has already been demonstrated that the photorefractive process in $BaTiO_3$ is heavily dependant on beam diameter, intensity, and incidence angle [Ref. 23]. Laser coherence length and its effect on conjugation was one issue that Glaros had identified as affecting the performance of the proposed instrument [Ref. 2, p.34]. In addition, Sutton states that coherent light is necessary for optimal phase conjugation [Ref. 24]. Single-line laser mode, necessary for higher coherence lengths, had not been used for the initial experiments due to the cost of retrofitting the available laser with an etalon assembly. Phase conjugation was still observed, however, and it may be conjectured that the high power levels used were enough to compensate for the lack of coherence in the light reaching the crystal. As a test of this theory, a 0.015 W argon-ion laser was obtained that was set up for single mode operation with an etalon.

Although this laser had less than 1/100 the power of the original laser, phase conjugation was still observed (Figure

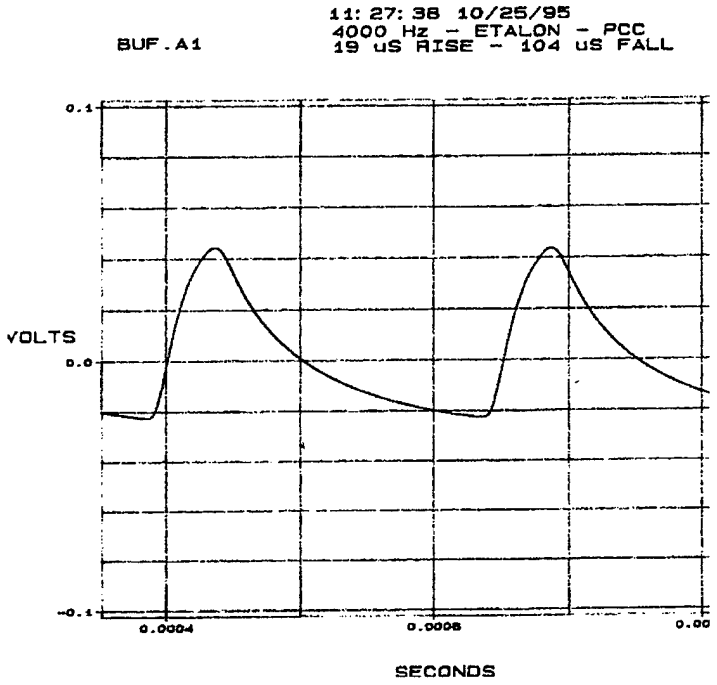

Figure 4.1 System Response with 15 mW single mode laser and PCM

4.1), and the diode output power levels were similar, although the output was not the desired square wave. This appears to corroborate the theory that single mode operation is far more efficient at producing a conjugate beam, but that this can be compensated for by substantially increasing the laser power.

While the 15 mW laser was producing conjugation, the lack of a square wave output from the PCM was a significant problem. One possible cause of this was a non-uniform laser beam entering the optical chopper, producing a nonlinear output at the diode. As a check on the single-mode laser beam uniformity, a conventional mirror was used in place of the

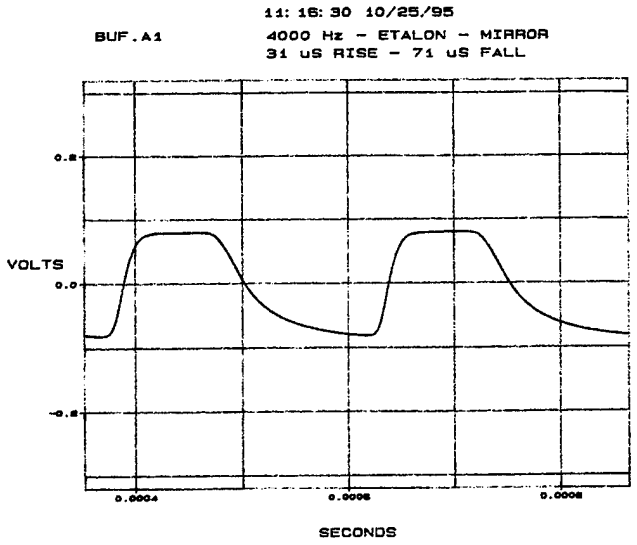

Figure 4.2 System Response with 15 mW single mode laser and conventional mirror

PCM. This was done to verify that the chopper was producing a symmetrical square wave. As seen in Figure 4.2, the rise and fall times were significantly different. In addition, the rise and fall slopes were not linear, indicating significant variations in power reaching the detector. Two possible causes of this are detector lag and uneven beam intensity. As

the detector has a response time less than 1/1000 that of the chopping frequency, it was conjectured that variations in beam intensity profile were producing this effect. Although the 0.015 W single line laser produced conjugation, the non-uniformity of the beam and the uneven power outputs produced as the chopper crossed the beam made it unsatisfactory. Therefore, the original 2 W argon-ion laser continued to be used for the remainder of the experiments. The 2 W argon-ion laser appears to work better at its lower power levels, when only the primary wavelength is emitting, resulting in increased coherence length. This however, is only a temporary solution to the coherence problem. It will be necessary to use more coherent sources in future investigations.

Laser beam divergence was another area that was found to affect the performance of the instrument. As can be readily observed, the output beam diameter increases noticeably as the light passes through the instrument. A small part of this increase is due to divergence, a known characteristic of all lasers, while thermal blooming causes a more significant increase in beam area. These effects produce two undesirable results: incomplete beam chopping and loss of energy at the

diode. Due to the small chopper aperture size relative to the beam, the signal is never completely on or off, introducing a small error into the readings. After passing through the plume, a significant thermal blooming caused the beam to increase to approximately 143% of the detector area. This effect was also noted by Glaros [Ref. 2, p. 28]. Increases in diameter can cause losses at the PCM and at the diode because of their small areas, reducing the amount of light that is measured. One way to counteract this would be through the use of a larger diode, possibly composed of several smaller units. In this way, the fast response time of the smaller diodes would be retained, while eliminating signal loss due to blooming. Another possible method to control the beam diameter is to use a photographic type aperture following the chopper to set a constant diameter of the beam, coupled with lenses to focus the beam. This would be done primarily to obtain a uniform beam for transmission, as Son *et al* [Ref. 3, p. 93] demonstrated that photorefractive conjugation is actually more likely with an increased beam diameter. Focusing lenses just before the diode were used in this investigation to minimize the effects of divergence.

An initial set of 21 calibration runs provided a baseline to evaluate system performance and repeatability. Cooling air was typically run at a high flow rate in order to protect the combustor against overheating. With these high cooling air flow rates, the ratio of combustion air to ethylene had to be set unusually low in order to maintain the flame. A mass flow ratio r ($r = \frac{\dot{m}_{air}}{\dot{m}_{fuel}}$) of 1/1 to 0.6/1 was used in order to determine how this ratio affected transmittance. The stochiometric ratio for air and etheylene is 14.7/1. As seen in Figure 3.4, a significant percentage of the cooling air flows into the central combustion tube, possibly reacting with the ethylene and also having an effect on the soot formation process through afterburning. Because of this, the cooling air to ethylene mass flow ratio was also varied, going from 13.3/1 to 6/1 to evaluate its effect on transmittance, with the assumption that this ratio would dominate the results.

The runs were broken down into seven different fuel-air ratios, with three runs made at each setting to determine if the instrument was producing repeatable results. All runs reflected good agreement between the pre-run and post-run

scene and reference beam intensities, indicating that there were no vibrations or other effects causing misalignments resulting in beam displacement from the diode. Transmittances were calculated from the ratio of scene beam to reference beam with and without particles, with the pre- and post-run intensity values averaged for the without-particle value. Based on this, the soot mass flow rate was calculated using Equation 2-9 and the flow velocities given in Table 3.2. Run results are shown in Table 4.1, with summaries in Figures 4.3 and 4.4

RUN	TotalAir/C_2H_4 mass flow ratio (r)	Combustion Air/C_2H_4 mass flow ratio (r)	Transmittance (%)	Soot Mass Emission Rate (kg/min)
1	13.3/1	1.3/1	91.2	1.64e-6
2	13.3/1	1.3/1	88.0	2.01e-6
3	13.3/1	1.3/1	86.4	2.30e-6
4	10/1	1/1	79.3	2.94e-6
5	10/1	1/1	80.0	2.83e-6
6	10/1	1/1	84.5	2.13e-6
7	10/1	0.75/1	84.6	2.14e-6
8	10/1	0.75/1	87.6	1.68e-6
9	10/1	0.75/1	75.2	3.62e-6
10	8/1	1/1	77.4	2.47e-6
11	8/1	1/1	79.6	2.20e-6
12	8/1	1/1	78.2	2.37e-6
13	8/1	1.3/1	78.3	2.36e-6
14	8/1	1.3/1	74.3	2.88e-6
15	8/1	1.3/1	81.4	1.99e-6
16	8/1	0.6/1	68.0	3.72e-6
17	8/1	0.6/1	80.8	2.06e-6
18	8/1	0.6/1	76.4	2.60e-6
19	6/1	0.6/1	66.3	3.79e-6
20	6/1	0.6/1	77.2	1.90e-6
21	6/1	0.6/1	71.6	2.46e-6

Table 4.1 Soot Mass Emission Rates at Varying Combustion Conditions

The groupings of three runs at each ratio showed good results, with no more than 41% difference between any group of three runs and most runs falling in a 20% deviation. This indicated that the instrument was producing repeatable readings at each combustion condition, as some of the variation was due to differences in the combustor itself. Finally, as seen in Figure 4.3, the transmittance showed good

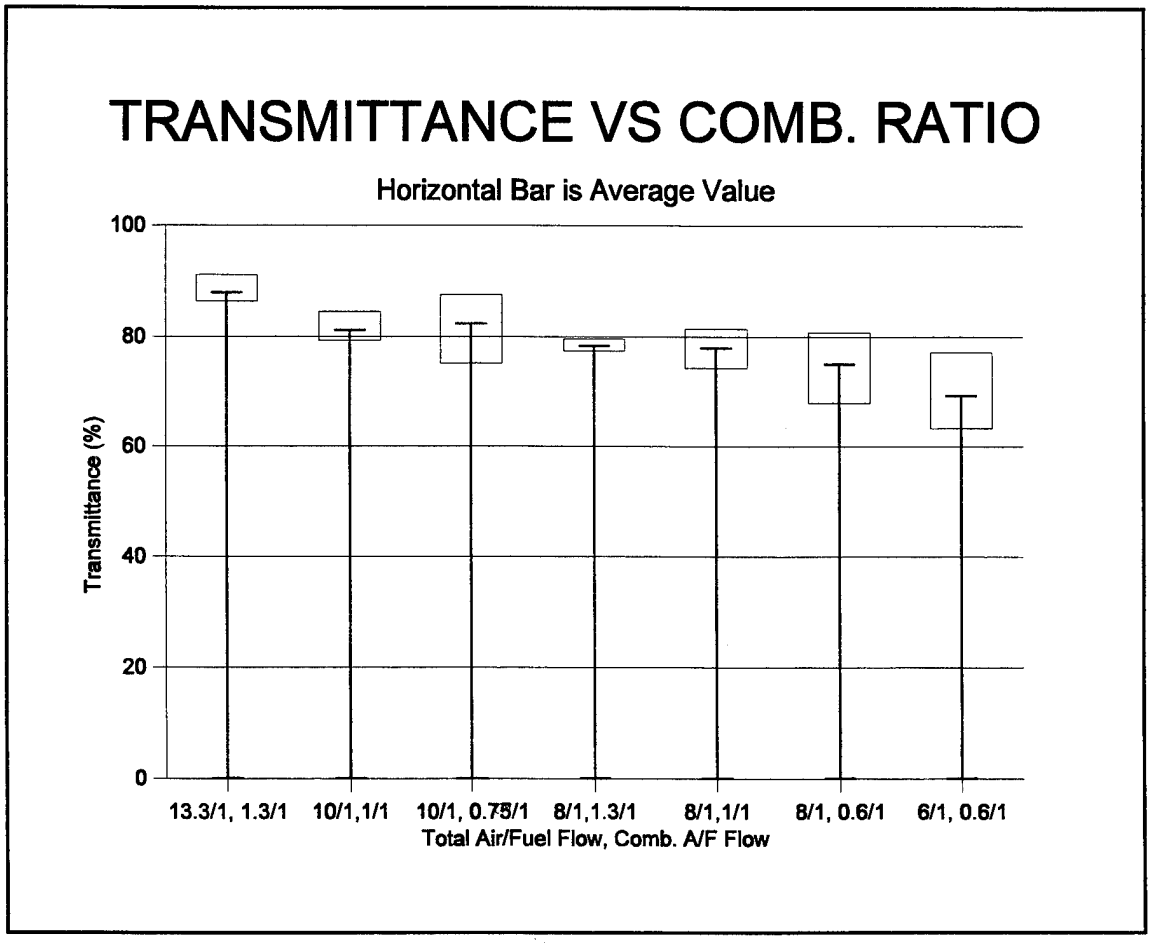

Figure 4.3 Combustion Transmittances

correlation with the ratio of overall air flow to ethylene, increasing steadily as more air was introduced into the combustor. Some of this effect was due to increased dilution of the soot by the increased air flow out the combustor exhaust, with the remainder being caused by the decrease in unburned soot due to more complete combustion. Calculating the soot mass flow rate eliminates the dilution as the air flow velocity was included in the calculations. These are shown in Figure 4.4 (flow in mg/min).

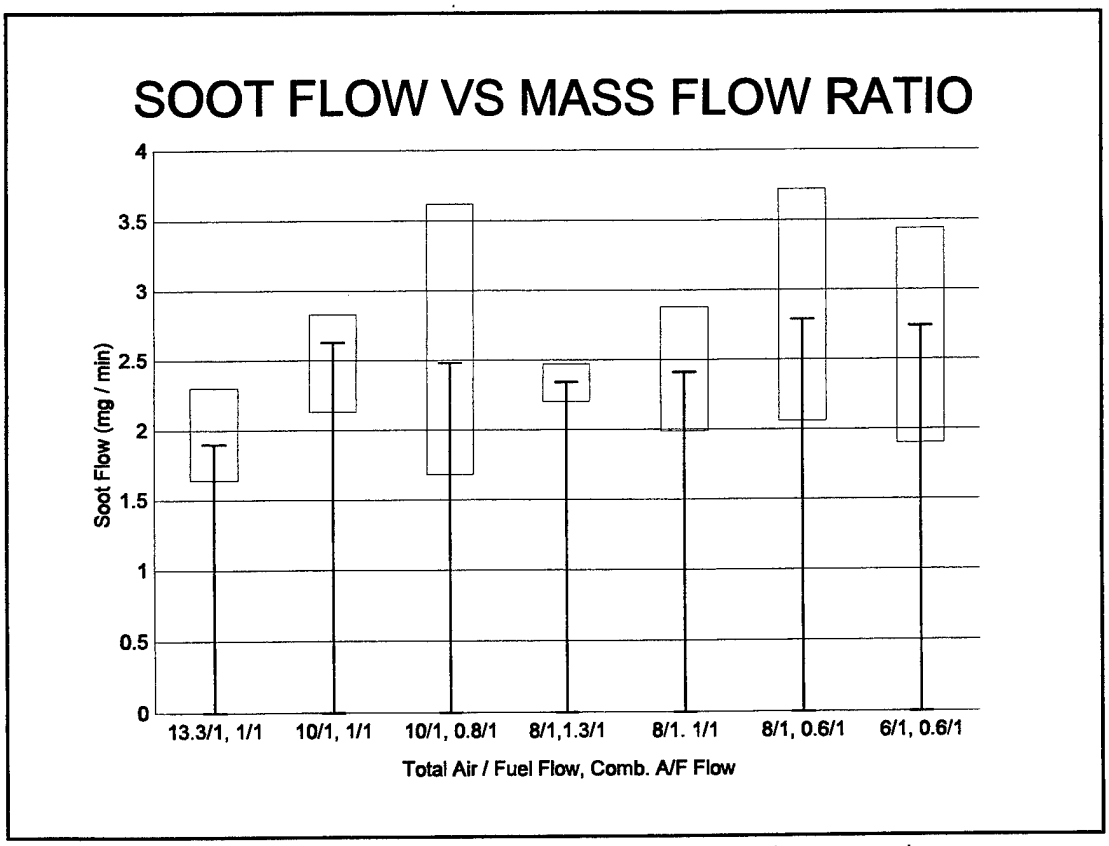

Figure 4.4 Soot Flow vs Combustion Ratio

The combustion air flow rate did not appear to have a great effect on the measured soot mass flow rate. This was due to the small magnitude relative to the total air flow and the C_2H_4 flow rates. Also, the total air contributed to combustor afterburning, which had a greater effect on the soot formation process. As a consequence of this, the data was averaged for the various values of total air flow only, with the results as shown in Figure 4.5. Although the data was internally consistent, there remains a variation between the

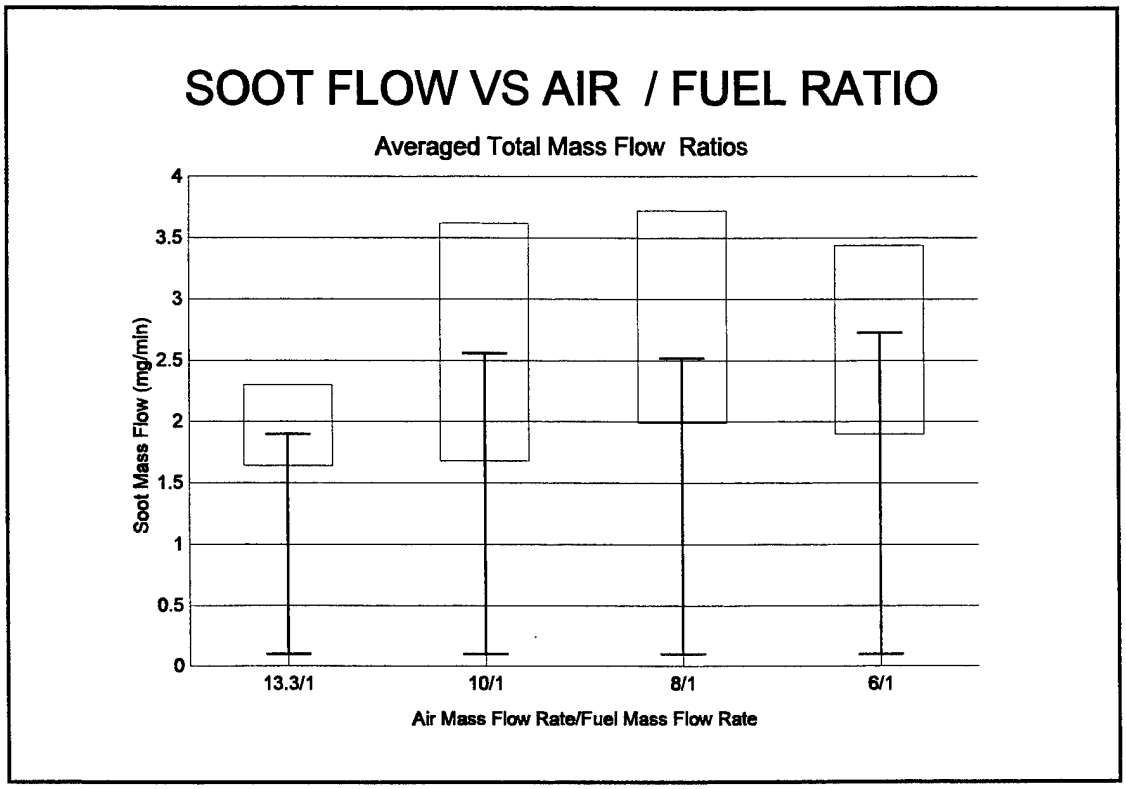

Figure 4.5 Averaged Soot Flow Rates

laser extinction results and those obtained with the sampling probe. Mass flow rate calculated using the collection method (Table 3.1) was approximately 30% of the flow rate calculated with the laser extinction method. One possible cause of this disparity is the relatively primitive sampling probe employed. As a test of this hypothesis, a larger fan was fitted to increase the sample probe flow rate, which appeared to be substantially less than the flow velocity in the duct. Three runs were conducted, with the results shown in Table 4.2 below:

RUN	TRANSMITTANCE (%)	SAMPLE MASS CHANGE (G)	EXTINCTION MASS FLOW RATE (KG/MIN)	SAMPLED MASS FLOW RATE (KG/MIN)
1	80.75	.0030	3.18e-6	1.2e-6
2	90.20	.0030	1.00e-6	1.2e-6
3	86.59	.0026	1.38e-6	1.0e-6

Table 4.2 Modified collection probe

As can be seen from above, there is still some difference between the calculated and collected mass flow rates, the largest single contributor to this being the uncertainties in building and operating the probe sampler. Even with the more

powerful exhaust fan, probe velocities were less than iso-kinetic, reducing the soot flow into the sample collection apparatus and the soot mass flow rate calculated from collected mass. While this is believed to be the primary cause of the disparity, several other factors could possibly affect the results. An extinction length of 0.127 meters was used, based on the observation that the beam was passing through the center of the plume only once, effectively making it a two-pass design. If the beam is actually passing through the plume four times, all of the above calculated results would be half their indicated value. The minute soot mass collected also introduces experimental uncertainties. A true iso-kinetic sampling system would give greater accuracy, and an operational unit would collect significant quantities of soot for measurement, reducing the uncertainties that have affected the comparison between the two methods.

V. CONCLUSIONS AND RECOMMENDATIONS

The four-pass instrument has been demonstrated in a simulated test cell environment. Further evaluation and development of the instrument will be necessary, but the underlying principles appear to be well understood. The greatest single obstacle found initially was obtaining reliable PCM operations at higher chopper speeds. While there is still a remote possibility that this was an inherent problem with the PCM, it is more likely that it was caused by the less than optimal operating characteristics of the lasers used. The only true way to test this is to obtain a single line laser with >1 Watt power, tuned to the optimum frequency, and to repeat the experiment. A revised instrument layout appears to significantly reduce this problem, however, and use of the revised setup as a final design should largely eliminate these problems.

The issues dealing with non-uniformity of the laser beam have also been problematic, although they can be minimized by careful laser selection and should have less of an effect on overall instrument accuracy. Any laser used should have a beam with a Gaussian intensity profile. Two areas that will

require further development are optics and a software package that will allow a direct soot mass readout. A focusing system, or alternatively, a larger diode that would be unaffected by beam growth effects, would provide greater stability and simplify alignment. Data acquisition and automatic conversion to soot mass concentration are necessary for any final version of the instrument. Using PC-based software would allow the use of laptop computers, eliminating the requirement to include this component in the system design.

Specific recommendations include:

1. The fastest possible chopping frequency, or alternately a copper vapor laser, should be used. The copper vapor laser appears to be the better choice, as it eliminates some of the error sources associated with mechanical chopping.
2. Laser power may be as low as 5 mW and still function effectively, if the laser has an etalon installed. If single-frequency mode is not available, laser power should be > 2 W to ensure conjugation. Light intensity control would

allow for better control of output power.

3. Proposed design: As shown in Figure 3.6, the final design should use a relatively compact, single mode laser, with an extra mirror to keep the light entering the PCM vertically polarized. Alternatively, a Faraday rotator could be used to accomplish this with the added benefit of protecting the laser cavity from returning energy. This would prevent the PCM from causing power fluctuations that could affect the results. Positioning the chopper at the beamsplitter output also appeared to prevent these laser cavity power fluctuations.

4. A larger diode, possibly composed of several smaller, fast diodes should be used to ensure that beam growth does not affect the readings.

If the above recommendations are implemented, an operational prototype could be completed and measurements in an actual test cell conducted. Ideally, this instrument should be calibrated against a soot source producing a known mass concentration prior to each test-cell operation.

LIST OF REFERENCES

1. Biblarz, O. and Netzer, D.W., *Evaluation of UTSI-CLA Program on Optical Measurements of Turbine Engine Exhaust Particulate*, Naval Postgraduate School Technical Report, NPS-AA-94-001CR, January 1994. (Distribution limited to U.S. government agencies.)

2. Glaros, G., *Soot Particle Density Determination From a Laser Extinction Multipass Technique*, M.S. thesis, Naval Postgraduate School, 32 pages, September 1994.

3. Shenoy, A.S., *"The Attenuation of Radiant Energy in HotSeeded Hydrogen"*, PhD Dissertation, Georgia Institute of Technology, School of Nuclear Engineering, 164 pages (May, 1969).

4. Van de Hulst, H.C., *Light Scattering by Small Particles*, Dover Publications Inc., New York (1957/1981)

5. Zel'dovich, B.Ya., Pilipetsky, N.F., and Shkunov, V.V., *Principles of Phase Conjugation*, Springer-Verlag, Berlin (1985).

6. Kailasanath, K. and Roy, G.D., *"Computational Combustion: Approaches to a Complex Phenomenon"* Naval Research Reviews 2, (1995).

7. Reed, R.A., *"Summary of Al_2O_3 Plume Characteristics and Behavior"*, 31st JANNAF Plume Conference Meeting, October 1994.

8. Stull, R.V. and Plass, G.N., *Emissivity of Dispersed Carbon Particles"*, J. Opt. Soc. Am., 50, pp. 121 (February 1960).

9. Dehne, H.J., *"Design, Construction and Preliminary Test of an Automated Isokinetic Sampler for Evaluating Particulate Emissions from Aircraft Gas Turbine Engines"*, Acurex Corp. Report 79-32/EE (December 1979).

10. Willecke, K. and Baron P. eds., *Aerosol Measurement; Principles, Techniques, and Applications*, Van Nostrand Reinhold, New York (1989).

11. Dalzell, W.H. and Sarofim, A.J., *"Optical Constants of Soot and their Application to Heat Flux Calculations"*, J. Heat Transfer, 91, pp. 100 (1969).

12. Few, J.D., *Light Scattering Techniques*, Particulate Emission Technology Meeting, April 16-18, 1985, Monterey, CA.

13. Nussenzveig, H.M. and Wiscombe, W.J., *"Efficiency Factors in Mie Scattering"*, Physical Review Letters, Vol 45(18), pp. 1490-1494, November 1980.

14. Hirlman, E.D.,*"Nonintrusive Laser Based Particle Diagnostics"*. AIAA Progress in Aeronautics and Astronautics, 92, 1984

15. Wade, R.A., Gore, J.P., and Sirvatham, Y.R., *"Soot Volume Fraction and Temperature Properties of High Liquid Loading Spray Flames"*, Combustion Institute; Chemical and Physical Processes in Combustion, 1993 Technical Meeting , Princeton N.J., October 25-27, 1993.

16. Dobbins,R.A.,Santoro,R.J.,and Semerjian,H.G.,*"Interpretation of the Optical Measurements of Soot"*, AIAA Progress in Aeronautics and Astronautics, 92 (1984).

17. Cashdollar, K.L., Lee, K.L., and Singer, J.M., *"Three Wavelength Light Transmission Technique to Measure Smoke Particle Size and Concentration"*, Applied Optics, 18, pp. 1763 (1 June 1979).

18. Few, J.D. and Hornkohl, J.O., *"Measurement and Prediction of Jet Engine Particulate effluents"*, Report No. NAPC-PE-195C, (February 1990).

19. Yeh, P., *"Photorefractive Phase Conjugators"*, IEEE Proceedings, Vol 80(3), March 1992.

20. Fisher, R.A., *Optical Phase Conjugation*, Academic Press, New York (1983).

21. Almeida, P.A. and Srisuda, P.V., *"Phase Conjugation by Four-Wave Mixing in Nematic Crystals"*, European Conference on Optics Proceedings, 1500, pp. 34 (15 March 1991).

22. Pepper, D., Rockwell, D.A., and Dunning, Gilmore, J.D., *"Nonlinear Optical Phase Conjugation"*, 1990 IEEE Nonlinear Optics: Materials, Phenomena, and Devices, (September 1991).

23. Son. J.Y., Jeon, H.W., and Choi, S.S. *"Light Propagation in a Photorefractive $BaTiO_3$ Crystal"*, SPIE 1841, Nonlinear Optical Processes in Solids (1991).

24. Sutton. G.P., *"Investigations of Self Pumped Phase Conjugate Laser Beams and Coherence Length"*, Master's Thesis, Naval Postgraduate School, 43 pages, (March 1993).

INITIAL DISTRIBUTION LIST

		No. Copies
1.	Defense Technical Information Center Cameron Station Alexandria, Virginia 22304-6145	2
2.	Library, Code 52 Naval Postgraduate School Monterey, California 93943-5101	2
3.	Prof. Oscar Biblarz, Code AA/Bi Naval Postgraduate School Monterey, California 93943-5106	3
4.	Prof. David Netzer, Code AA/Nt Naval Postgraduate School Monterey, California 93943-5106	3
5.	Chairman Space Systems Academic Group Naval Postgraduate School Monterey, California 93943-5106	1
6.	Chairman Department of Aeronautics and Astronautics Naval Postgraduate School Monterey, California 93943-5106	1
7.	Mr Donald Lincoln Counsel, Code 006 Naval Postgraduate School Monterey, California 93943-5106	2
8.	Mr William Vorhees Code PE34 Naval Air Warfare Center, Aircraft Division Trenton, New Jersey 08628-0176	4
9.	LT Philip Turner 127 Maple Street New Providence, New Jersey 07974	4